MINISTRY OF EDUCATION
AND TRAINING

VIETNAM ACADEMY
OF SCIENCE AND TECHNOLOGY

GRADUATE UNIVERSITY OF SCIENCE AND TECHNOLOGY

------------ *** ------------

NGUYEN TUAN DUY

THE EFFECT OF SCALAR FIELDS ON THE FLAVOR-CHANGING NEUTRAL CURRENTS IN THE S331 MODEL AND 3-3-1-1 MODEL

SUMMARY OF MATERIALS SCIENCE DOCTORAL THESIS

HA NOI – 2023

The thesis was completed at: Department of Physics, Graduate School of Science and Technology - Vietnam Academy of Science and Technology

Supervisors : Prof. Dr. Phung Van Dong
              Assoc.Prof. Dr. Do Thi Huong

Referee 1 : Assoc.Prof. Dr. Tran Minh Hieu
Referee 2: Assoc.Prof. Dr. Phan Hong Lien
Referee 3: Dr. Cao Hoang Nam

The thesis was defended in front of the doctoral thesis grading committee, meeting at the Graduate School of Science and Technology - Vietnam Academy of Science and Technology at 9 am, 17th May, 2023

The thesis can be found at:
- Library of Academy of Science and Technology;
- Vietnam National Library.

INTRODUCTION

1. The urgency of the thesis

The Standard Model (SM) is currently considered as the orthodox theory to describe elementary particle interactions. Several SM predictions, including the existence and properties of c, t quarks, and gauge bosons $W^{\pm}$ and Z, were experimentally confirmed with high precision.The discovery of the Higgs boson at the LHC in 2012 is considered the final piece of the Standard Model picture. However, there are many more issues that SM cannot solve, such as not explaining why the number of fermion generations is equal to 3, the neutrino masses, dark matter, dark energy, CP violation in QCD, and matter-antimatter asymmetry. This implies that SM cannot be the end of line. Particle physicists have been inspired to propose many BSM in which new physics states present at TeV-scale.The signals of these BSM are searched for at the accelerator as new resonances or as deviations from the SM prediction in specific observables. In recent years, the process of modifying the predicate has garnered the most attention, as improvements in both nonperturbative techniques and data analysis have begun to reveal differences between the SM prediction and the experimental one. These $2 - 4\sigma$ deviations are known as flavor anomalies.There are assumptions that these anomalies arise as a result of our incomplete understanding of the non-perturbation effect, but in general, they are strongly implied about the origin of the new physics due to the large deviation and being very difficult to explain by SM itself.

There are three methods to build BSM models: via extending the spacetime dimension, the particle spectrum, and the electroweak gauge symmetry group. In this thesis, we investigate current anomalies in two BSM model electroweak symmetry group extension: the simple 3-3-1 model (S331) and the 3-3-1-1 model. The 3-3-1 model is based on the gauge group $SU(3)_C \otimes SU(3)_L \otimes U(1)_X$, which explains a number of SM issues, including the family number, charged

quantization, neutrino masses, CP violation in QCD, and dark matter. The 3-3-1 models can be separated into numerous variants based on the arrangement of particle spectrum and the number of Higgs multiplets, whereas S331 model receiving the most attention. It carries a unique Higgs spectrum featuring interactions at the tree level of the Higgs triplet with both leptons and quarks via generic Yukawa matrices, which are the source of lepton (quark) flavor violation decays of Standard Model like the Higgs boson (SMLHB), $h \to l_i l_j$, $h \to q_i q_j (i \neq j)$, FCNC of the top quark $t \to qh$ $(q = u, c)$, anomalous magnetic moment of the muon a_μ. In addition, the meson mixing systems $\Delta m_K, \Delta m_{B_s}, \Delta m_{B_d}$ receive contributions from the new Higgs in addition to the contributions from the known gauge bosons.

The model, which is based on the gauge group $SU(3)_C \otimes SU(3)_L \otimes U(1)_X \otimes U(1)_N$ (3-3-1-1 model), is an extension of the 3-3-1 model with a gauged $B-L$ symmetry, which not only inherits the advantages of 3-3-1 model but also has a naturally stable mechanism for dark matter, explains the inflation problem, matter-antimatter asymmetry. In this model, there have been several phenomenological studies, one of which is the study of the FCNC process in meson mixing systems $\Delta m_K, \Delta m_{B_s}, \Delta m_{B_d}$. However, only the FCNC contribution associated with the new gauge boson Z_2, Z_N is taken into account, and not the FCNC of the new scalars. In addition, the FCNC contributions influence rare decay of B meson such as $B_s^0 \to \mu^+ \mu^-$, $B \to K^* \mu^+ \mu^-$, and $B^+ \to K^+ \mu^+ \mu^-$ at the tree level. The 3-3-1-1 model additionally predicts new charged Higgs and new charged gauge bosons, and this is a new contributor to lepton and quark flavor violation decays, such as $b \to s\gamma$, $\mu \to e\gamma$.

For the aforementioned reasons, we chose the topic "The effect of scalar fields on the flavor-changing neutral currents in the S331 model and 3-3-1-1 model."

2. The objectives of the thesis

- In the S331 model, based on the lepton and quark flavor violation interactions of Higgs triplets, there are some phenomenologies studied, such as the LFVHD and QFVHD $h \to l_i l_j, h \to q_i q_j$ $(i \neq j)$, cLFV decay $\tau \to \mu\gamma$, anomalous magnetic moment of the muon a_μ, FCNC top quark decay $t \to qh$. Also presented is the new contribution of the scalar component to the meson mixing systems: $\Delta m_K, \Delta m_{B_s}, \Delta m_{B_d}$.

- In the 3-3-1-1 model, the study of FCNC-associated anomalies receives new contributions from the scalar part of meson mixing systems $\Delta m_K, \Delta m_{B_s}$,Δm_{B_d} and several rare decays of B meson: $B_s \to \mu^+\mu^-$, $B \to K^{(*)}\mu^+\mu^-$.

3. The main contents of the thesis

- The overview of SM and some BSM models. We present some of the most recent experimental constraints and flavor anomalies discovered in colliders.

- The summary of the S331 model. We consider the influences of lepton and quark flavor violating interactions of Higgs triplets in some processes, namely LFVHD and QFVHD, cLFV decay, anomalous muon magnetic moment, FCNC top quark decay, and meson mixing systems.

- The summary of the 3-3-1-1 model. The contributions from new scalars into phenomenologies associated with FCNC include meson mixing systems, rare decays of B meson, and flavor violating radiative decays contributed by newly charged Higgs and gauge bosons.

CHAPTER 1. OVERVIEW

1.1. The Standard Model

The SM of elementary particle physics is a renormalizable quantum field theory that describes three of the four known interactions of nature, with the exception of gravity. The particle spectrum in SM is represented as follows:

$$\text{Leptons}: \ \psi_{\alpha L} = \begin{pmatrix} \nu_{\alpha L} \\ e_{\alpha L} \end{pmatrix} \sim (1, 2, -1), \qquad e_{\alpha R} \sim (1, 1, -2),$$

$$\text{Quarks}: \ Q_{\alpha L} = \begin{pmatrix} u_{\alpha L} \\ d_{\alpha L} \end{pmatrix} \sim (3, 2, 1/3),$$

$$u_{\alpha R} \sim (3, 1, 4/3), \qquad d_{\alpha R} \sim (3, 1, -2/3), \tag{1.1}$$

where $\alpha = 1, 2, 3$ are the generation indexes.

In order to generate particle masses, SM must be spontaneously symmetry broken (SSB) or demand the Higgs mechanism. The Higgs mechanism works with the following doublet

$$\phi = \begin{pmatrix} \varphi^+ \\ \varphi^0 \end{pmatrix} \sim (1, 2, 1), \qquad \phi_0 = \frac{1}{\sqrt{2}} \begin{pmatrix} 0 \\ v \end{pmatrix}. \tag{1.2}$$

After SSB, we have gauge bosons $W_\mu^\pm, Z_\mu, A_\mu$ with masses and eigenstates defined in the thesis Lagrangian Yukawa $\mathcal{L}_Y^{\text{lepton}}$ for leptons is

$$\mathcal{L}_Y^{\text{lepton}} = -\sum_{a,b} \bar{e}_{aL} \mathcal{M}_{ab}^l e_{bR} + \bar{e}_{aL} \frac{\mathcal{M}_{ab}^l}{v} e_{bR} H + h.c., \tag{1.3}$$

with $\mathcal{M}_{ab}^l = \frac{h_{ab}^l}{\sqrt{2}} v$. This matrix can be diagonalized using two unitary matrices, V_L, V_R.

Lagrangian Yukawa for quarks is

$$\mathcal{L}_{\text{Yukawa}}^{\text{mass}} = -\sum_{a,b} \bar{u}_{aL} \mathcal{M}_{ab}^u u_{bR} + \bar{d}_{aL} \mathcal{M}_{ab}^d d_{bR}$$

$$-\sum_{a,b}\bar{u}_{aL}\frac{\mathcal{M}^u_{ab}}{v}u_{bR}H+\bar{d}_{aL}\frac{\mathcal{M}^d_{ab}}{v}d_{bR}H+h.c., \qquad (1.4)$$

with $\mathcal{M}^{u,d}_{ab}=h^{u,d}_{ab}\frac{v}{\sqrt{2}}$ is mixing quark mass matrices and can be diagonalized using unitay matrices $V^d_{L,R}, V^u_{L,R}$.

Next, we consider the interactions between leptons and gauge bosons. The charged current interactions have the following form:

$$\mathcal{L}^{\text{lepton}}_{CC}=g(J^1_\mu W^{1'}_\mu+J^2_\mu W^{2'}_\mu)\ =J^-_\mu W^{-\mu}+J^+_\mu W^{+\mu}, \qquad (1.5)$$

where the currents $J^\pm_\mu$ are defined as

$$J^+_\mu=\frac{g}{\sqrt{2}}\sum_{a=1,2,3}\bar{\nu}_{aL}\gamma_\mu e_{aL}, \qquad J^-_\mu=\frac{g}{\sqrt{2}}\sum_{a=1,2,3}\bar{e}_{aL}\gamma_\mu \nu_{aL}. \qquad (1.6)$$

The neutral and electromagnetic currents are

$$\mathcal{L}^{\text{lepton}}_{NC+em}\ =\ eJ^{\text{em}}_\mu A^\mu+\frac{g}{c_W}J^Z_\mu Z^\mu. \qquad (1.7)$$

with

$$J^Z_\mu=\sum_{a=1,2,3}\bar{l}_a\gamma_\mu[g_L P_L+g_R P_R]l_a, \qquad J^{\text{em}}_\mu=\sum_{a=1,2,3}Q(l)\bar{l}_a\gamma_\mu l_a, \qquad (1.8)$$

with $g_{L,R}=T_3(l_{L,R})-s^2_W Q(l)$.

We do it similarly for quark. The charged current interactions of quarks are

$$\mathcal{L}^{\text{quark}}_{CC}\ =\ \frac{g}{\sqrt{2}}\bar{u}'_{iL}\gamma^\mu V_{ij}d'_{jL}W^+_\mu+h.c., \qquad (1.9)$$

where $V=V^{u\dagger}_L V^d_L$ is an unitay matrix 3×3, the so called CKM matrix.

The electromagnetic and neutral currents of quarks

$$\mathcal{L}^{\text{quark}}_{\text{em}}=eJ^{\text{em}}_\mu A^\mu, \qquad J^{\text{em}}_\mu=\sum_{a=1,2,3}Q(q)\bar{q}_a\gamma_\mu q_a, \qquad q=u,d,$$

$$\mathcal{L}^{\text{quark}}_{NC}=\frac{g}{c_W}J^Z_\mu Z^\mu, \qquad J^Z_\mu=\sum_{a=1,2,3}\bar{q}_a\gamma_\mu[g_L P_L+g_R P_R]q_a. \qquad (1.10)$$

1.2. Current experimental constraints and flavor anomalies

1.2.1. LFVHD and QFVHD

Since the SM lacks right-handed neutrinos, the mass of Dirac neutrinos is zero. As a result, the lepton number is conserved, which prevents the appearance of the cLFV decay. Experiments have confirmed, however, that neutrinos

have mass and that they oscillate among generations. In the extended version of the Standard Model with right-handed neutrinos, ν_R, cLFV decay may exist but are heavily suppressed by the GIM mechanism $\mathrm{Br}(\mu \to e\gamma) < 10^{-54}$. Other cLFV decays, such as $\mu \to 3e, \tau \to (e, \mu)\gamma$, similarly have extremely small branching ratios, and none of the present experiments have enough sensitivity to measure this value. Currently, it is not established which cLFV signal is observed experimentally; rather, the upper limit of the branching ratio is given, namely $\mathrm{Br}(\mu \to e\gamma) < 4.2 \times 10^{-13}$ (MEG experiment), $\mathrm{Br}(\tau \to e\gamma) < 3.3 \times 10^{-8}$, $\mathrm{Br}(\tau \to \mu\gamma)$ (Babar experiment) with 90% confidence level.

New physics may also manifest as Higgs boson properties different than those anticipated by SM, such as the LFVHD $h \to l_i l_j$ $(i \neq j)$. In SM, only lepton-conserving decays $h \to f\bar{f}$ are allowed, whereas LFVHDs $h \to l_i l_j$ $(i \neq j)$ are not permitted. Current experimental limits for these LFVHDs are $\mathrm{Br}(h \to e\mu) < 6.1 \times 10-5$, $\mathrm{Br}(h \to \mu\tau) < 2.5 \times 10^{-3}$, and $\mathrm{Br}(h \to e\tau) < 4.7 \times 10^{-3}$. This shows that this may be an indication of the new physics.

1.2.2. *The anomalous muon magnetic moment*

The SM prediction for the anomalous muon magnetic moment a_μ^{SM} is

$$a_\mu^{\mathrm{SM}} = 116591810(43) \times 10^{-11}, \tag{1.11}$$

The very recent experiment result for a_μ by $g-2$ experiment at FNAL reads

$$a_\mu^{\mathrm{Exp}} = 116\ 592061(41) \times 10^{-11} \tag{1.12}$$

and shows the deviations with the SM one about 4.2σ

$$\Delta a_\mu \equiv a_\mu^{\mathrm{Exp}} - a_\mu^{\mathrm{SM}} = 251(59) \times 10^{-11}. \tag{1.13}$$

The impressive accuracy of the SM prediction and experimental measurement provide a_μ a highly accurate physics observable and one of the most sensitive channels for searching for a new physics signal. If new physics is required to explain this Δa_μ discrepancy, it would appear in one-loop diagram contributions (new scalars, new vectors, or new fermions).

1.2.3. *FCNC top quark decay* $t \to qh$ $(q = u, c)$

New physics effects are possible in the quark sector, but they are considerably complicated by interactions that contradict the Higgs predicate for the

top quark. The decays $t \to qh$ with $q = u, c$ are one of the top-quark FCNC processes. In the SM, Br$(t \to ch) \simeq 10^{-15}$, Br$(t \to uh) = |V_{ub}/V_{cb}|^2Br(t \to uh) = |V_{ub}/V_{cb}|^2Br(t \to uh) \simeq 10^{-17}$ are extremely small. Currently, CMS and ATLAS have not found any significant signals against the background for FCNC decays of top quarks, leading to upper limits for the branching ratios Br$(t \to qh) < 0.47\%$ with a confidence level of 95%.

1.2.4. The anomalies in semi-leptonic decays of B meson

A crucial prediction of the SM is that different generations of charged leptons exhibit the same interaction (lepton flavor universality-LFU). Nonetheless, a few recent experiments have revealed the violation of LFU (LFUV), suggesting that it may be an indication of new physics. One of the LFUV signals occurs in the FCNC quark transitions $b \to sl^+l^-$ ($l = e, mu$) of the B meson, which differs from the prediction of the Standard Model $\sim 3\sigma$: e.g. branching ratio Br$(B^+ \to K^+\mu^+\mu^-)$, Br$(B^0 \to K^{0*}\mu^+\mu^-)$, Br$(B_s^0 \to \phi\mu^+\mu^-)$; the P_5' coefficient in the decay $B^0 \to K^{0*}\mu^+\mu^-$. Due to the GIM mechanism, these LFUV observables cannot occur at the tree-level in the SM and are only present when considering the quantum corrections, such as penguin or box diagrams.

1.3. BSMs

1.3.1. Minimal left-right symmetry model

The minimal left-right symmetry model (MLRSM) has the norm group $SU(3)_C \otimes SU(2)_L \otimes SU(2)_R \otimes U(1)_{B-L}$ as one of the models. The earliest BSM model was studied. This model was originally built to explain the observed parity asymmetry in the weak interaction through group symmetry breaking $SU(2)_R$ on the energy scale. High. This is also the first model to explain the small mass of neutrinos through the seasaw mechanism thanks to the presence of right-biased neutrinos ν_R. However MLRSM does not solve the problem of dark matter, like SM.

1.3.2. 3-3-1 models

One of the most popular BSM models in which the standard group is of the form $SU(3)_C \otimes SU(3)_L \otimes U(1)_X$ (abbreviated as 3-3-model) first). The main motivation for building this kind of 3-3-1 model was to answer the question of

why it is observed in nature that there are three generations of matter through the relationship between the number of generations and the cancellation of the $[SU(3)_L]^3$ anomaly. Many problems of SM are well solved by this model: neutrino mass, charge quantization, number of matter generations, unusually heavy mass of top quark, CP violation in QCD, dark matter. Besides, this type of model has other advantages such as the mathematical structure is not too complicated compared to other BSM models such as SUSY, extra-dimensional models. The new physics scale of the 3-3-1 is not too large, so it can be experimentally verified at an accelerator such as the High Luminosity-LHC (HL-LHC) project being upgraded at the LHC or the international linear collider (ILC) is being proposed. Importantly, the 3-3-1 models contain non-trivial fermion contents under the $SU(3)_L$ symmetry, thus providing direct predictions for anomalies related to the lepton and quark flavors.

1.3.3. 3-3-1-1 models

Recently, Phung Van Dong and team showed an extension of SM in which the standard symmetry is extended to the group $SU(3)_C \otimes SU(3)_L \otimes U(1)_X \otimes U(1)_N$, which is called the 3-3-1-1 model. This model contains both the mathematical and phenomenological aspects of the 3-3-1 model. Therefore, the 3-3-1-1 pattern has all the advantages of the 3-3-1 model. The difference between the 3-3-1-1 model and the 3-3-1 models is the nature of the $B - L$ symmetry. In the 3-3-1-1 model, the symmetry $B - L$ is understood as a gauge symmetry that is not commutative with 3-3-1 symmetry. Therefore, there will be a unification between the electromagnetic interaction and the $B - L$ interaction, like the theory of Glashow-Weinberg-Salam. In addition, this model also provides a natural, comprehensive explanation for neutrino mass, dark matter, cosmic inflation, and matter-antimatter asymmetry.

2.1. The summary of the S331 model

The S331 model is a combination of the reduced minimal 3-3-1 model and the minimal 3-3-1 model. This model contains the following fermion spectrum:

$$\psi_{aL} \equiv \begin{pmatrix} \nu_{aL} \\ e_{aL} \\ (e_{aR})^c \end{pmatrix} \sim (1,3,0), \quad Q_{\alpha L} \equiv \begin{pmatrix} d_{\alpha L} \\ -u_{\alpha L} \\ J_{\alpha L} \end{pmatrix} \sim (3,3^*,-1/3)$$

$$Q_{3L} \equiv \begin{pmatrix} u_{3L} \\ d_{3L} \\ J_{3L} \end{pmatrix} \sim (3,3,2/3), \quad u_{aR} \sim (3,1,2/3)$$

$$d_{aR} \sim (3,1,-1/3), \quad J_{\alpha R} \sim (3,1,-4/3), \quad J_{3R} \sim (3,1,5/3) \quad (2.1)$$

with $a = 1,2,3$ and $\alpha = 1,2$ are the generation indexes. The third generation of quarks is arranged differently than the first two generations in order to obtain acceptable FCNC when the energy scale of the S331 model is suppressed by the Landau pole. The scalar spectrum is

$$\eta = \begin{pmatrix} \eta_1^0 \\ \eta_2^- \\ \eta_3^+ \end{pmatrix} \sim (1,3,0), \quad \chi = \begin{pmatrix} \chi_1^- \\ \chi_2^{--} \\ \chi_3^0 \end{pmatrix} \sim (1,3,-1), \quad (2.2)$$

with VEVs read $\langle \eta_1^0 \rangle = \frac{u}{\sqrt{2}}, \langle \chi_3^0 \rangle = \frac{w}{\sqrt{2}}$. In order to reveal candidates for DM, an inert scalar multiplet $\phi = \eta', \chi'$ or σ is added. Lagrangian Yukawa reads

$$\begin{aligned} \mathcal{L}_Y &= h_{33}^J \bar{Q}_{3L} \chi J_{3R} + h_{\alpha\beta}^J \bar{Q}_{\alpha L} \chi^* J_{\beta R} + h_{3a}^u \bar{Q}_{3L} \eta u_{aR} + \frac{h_{\alpha a}^u}{\Lambda} \bar{Q}_{\alpha L} \eta \chi u_{aR} \\ &\quad + h_{\alpha a}^d \bar{Q}_{\alpha L} \eta^* d_{aR} + \frac{h_{3a}^d}{\Lambda} \bar{Q}_{3L} \eta^* \chi^* d_{aR} + h_{ab}^e \bar{\psi}_{aL}^c \psi_{bL} \eta \\ &\quad + \frac{h_{ab}'^e}{\Lambda^2} (\bar{\psi}_{aL}^c \eta \chi)(\psi_{bL} \chi^*) + \frac{s_{ab}^\nu}{\Lambda} (\bar{\psi}_{aL}^c \eta^*)(\psi_{bL} \eta^*) + h.c., \quad (2.3) \end{aligned}$$

9

2.2. LFV interactions of Higgs

2.2.1. $h \to \mu\tau$

Lagrangian for LFV interactions of Higgs reads

$$
\begin{aligned}
\mathcal{L}_Y \supset\ & \bar{e}'_R g_h^{ee} e'_L h + \bar{e}'_R g_H^{ee} e'_L H \\
& + \left\{ (\bar{e'_L})^c g_L^{e\nu} \nu'_L + (\bar{\nu'_L})^c g_L^{\nu e} e'_L + \bar{\nu}'_L g_R^{\nu e} e'_R + (\bar{e'_R})^c g_R^{e\nu} (\nu'_L)^c \right\} H^+ + h.c.,
\end{aligned}
$$
$$(2.4)$$

with $g_h^{ee} = U_R^{e\dagger} \left(c_\zeta \frac{1}{u} \mathcal{M}_e - s_\zeta \frac{uw}{\sqrt{2}\Lambda^2} h'^e \right) U_L^e$, $g_H^{ee} = U_R^{e\dagger} \left(s_\zeta \frac{1}{u} \mathcal{M}_e + c_\zeta \frac{uw}{\sqrt{2}\Lambda^2} h'^e \right) U_L^e$,
$g_L^{e\nu} = (U_L^e)^T \left(c_\theta\, h^e + s_\theta \frac{uw}{2\Lambda^2} h^{e\prime} \right) U_L^\nu$, $g_L^{\nu e} = (U_L^\nu)^T c_\theta h^e U_L^e$, $g_R^{\nu e} = U_L^{\nu\dagger} c_\theta \frac{u}{\sqrt{2}\Lambda} s^\nu U_R^e$,
$g_R^{e\nu} = U_L^{eT} c_\theta \frac{u}{\sqrt{2}\Lambda} s^\nu U_R^{\nu T}$, $(\mathcal{M}_e)_{ab} = \sqrt{2} u \left(h_{ab}^e + \frac{h_{ab}'^e w^2}{4\Lambda^2} \right)$ is the mixing mass matrix of charged leptons. The branching ratio for the LFVHD is

$$
\mathrm{Br}(h \to e_i e_j) = \frac{m_h}{8\pi\Gamma_h} \left(|g_h^{e_i e_j}|^2 + |g_h^{e_j e_i}|^2 \right),
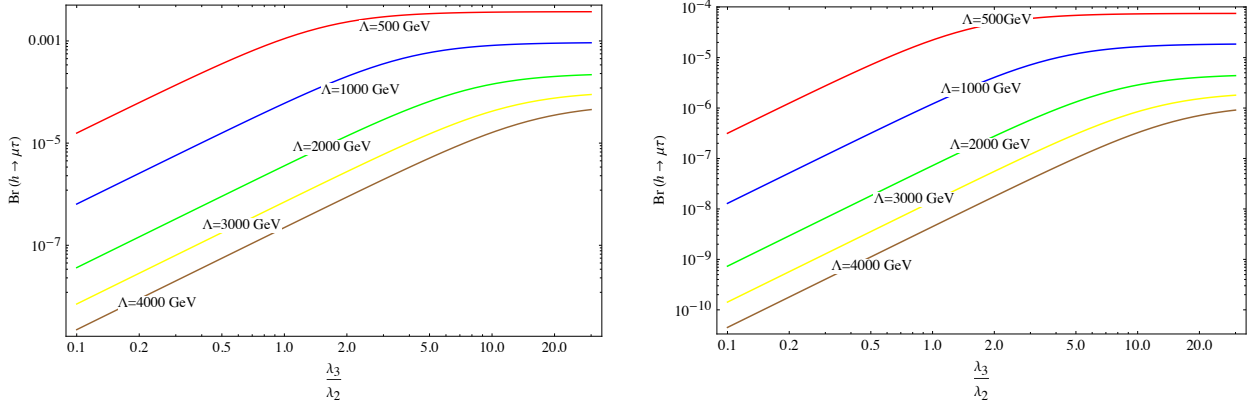$$
$$(2.5)$$

Figure 2.1: The branching ratio $\mathrm{Br}(h \to \mu\tau)$ is as the function of the factor $\frac{\lambda_3}{\lambda_2}$ with the different energy scale Λ. The left and right panel are plotted by fixing $\left[(U_R^e)^\dagger h'^e U_L^e \right]_{\mu\tau} = 2 \frac{\sqrt{m_\mu m_\tau}}{u}$, and $\left[(U_R^e)^\dagger h'^e U_L^e \right]_{\mu\tau} = 5 \times 10^{-4}$, respectively

In the small region of Λ and the factor $\frac{\lambda_3}{\lambda_2} > 1$, $\mathrm{Br}(h \to \mu\tau) \simeq 10^{-3}$. However, in this regime, S331 model may encounter the strong precision constraints of Higgs. If $\Lambda \sim$ TeV but still is below the Landau pole, $\lambda_1 \sim \lambda_2$, the mixing angle ξ will be small and $\mathrm{Br}(h \to \mu\tau) \simeq 10^{-5}$.

2.2.2. $\tau \to \mu\gamma$

The branching ratio of the cLFV decay $\tau \to \mu\gamma$ has the following form

$$\mathrm{Br}(\tau \to \mu\gamma) \quad = \quad \frac{48\pi^3\alpha}{G_F^2}\left(|D_L^\gamma|^2 + |D_R^\gamma|^2\right)Br(\tau \to \mu\bar{\nu}_\mu\nu_\tau), \qquad (2.6)$$

where the factors $D_{L,R}^\gamma$ are contributions from the one-loop and two-loop diagrams (see in the thesis for details)

We now numerically study the contribution of each type of diagram for the branching ratio of $\tau \to \mu\gamma$.
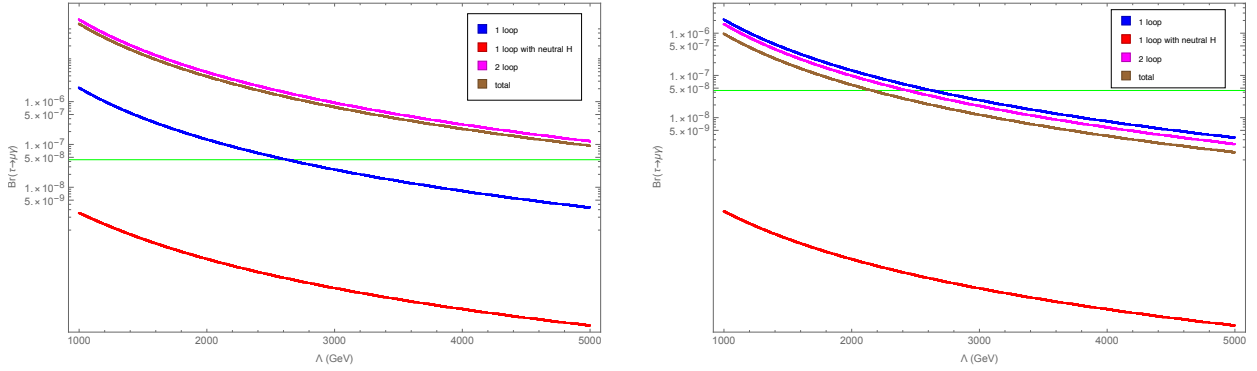
Figure 2.2: The dependence of $\mathrm{Br}(\tau \to \mu\gamma)$ on Λ with different contributions. The green line is the current experimental constraint $\mathrm{Br}(\tau \to \mu\gamma)_{\mathrm{Exp}} < 4.4 \times 10^{-8}$. We fix $\left[(U_R^e)^\dagger h'^e U_L^e\right]_{\mu\tau} = 2\frac{\sqrt{m_\mu m_\tau}}{u}$ and $\left[(U_R^e)^\dagger h'^e U_L^e\right]_{\mu\tau} = 5 \times 10^{-4}$, correspondingly for the left and right panel. The factor $\frac{\lambda_3}{\lambda_2} = 1$ is applied for both panels.

The results shown in the Fig. 2.2 indicate that the two-loop diagrams can be the primary contribution for $\tau \to \mu\gamma$. Depending on choice, $\left[(U_R^e)^\dagger h'^e U_L^e\right]_{\mu\tau} = 2\frac{\sqrt{m_\mu m_\tau}}{u}$, or $\left[(U_R^e)^\dagger h'^e U_L^e\right]_{\mu\tau} = 5 \times 10^{-4}$, the two-loop contributions to $\mathrm{Br}(\tau \to \mu\gamma)$ can be larger or smaller than the one-loop contributions. However, the scenario $\left[(U_R^e)^\dagger h'^e U_L^e\right]_{\mu\tau} = 5 \times 10^{-4}$ gives $\Lambda > 2.4$ TeV, in agreement with Landau pole limit. We compare Fig. 2.2 and Fig. 2.3, we find that the above statement changes slightly when the factor $\frac{\lambda_3}{\lambda_2}$ raises.

11

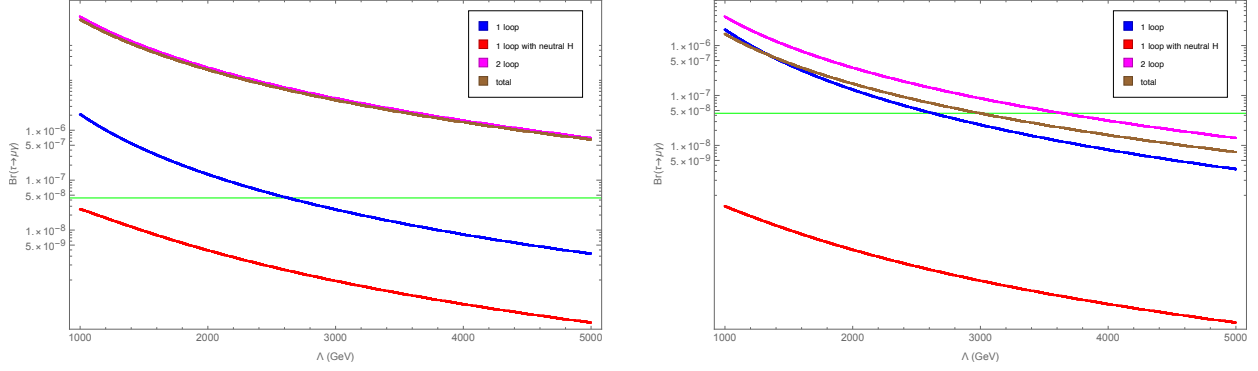Figure 2.3: $\mathrm{Br}(\tau \to \mu\gamma)$ when fixing $\frac{\lambda_3}{\lambda_2} = 5$

2.2.3. $(g-2)_\mu$

The S331 model contains FCNC, hence, it also contributes to the anomalous muon magnetic moment

$$(\Delta a_\mu)^{M331} \simeq \sum_\phi \left(g_\phi^{\tau\mu} \right)^2 \frac{m_\mu m_\tau}{8\pi^2 m_\phi^2} \left(\ln \frac{m_\phi^2}{m_\tau^2} - \frac{3}{2} \right). \qquad (2.7)$$
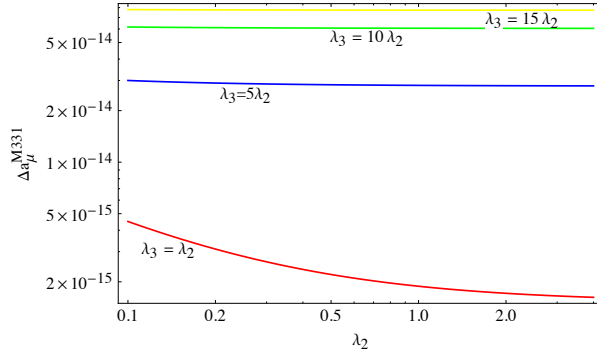

Figure 2.4: The contribution of LFV interactions of Higgs to Δa_μ^{M331} as the function of the Higgs coupling λ_2 with different factors $\frac{\lambda_3}{\lambda_2}$.

The Fig. 2.4 with the input parameters can explain the experimental constraint of $\mathrm{Br}(h \to \tau\mu)$ but cannot deal Δa_μ^{M331}. Nevertheless, $(g-2)_\mu$ in the S331 model also receives contribution from the doubly charged gauge boson

$$\Delta a_\mu(Y^{\pm\pm}) \simeq \frac{28}{3} \frac{m_\mu^2}{u^2 + w^2}. \qquad (2.8)$$

The energy scale that breaks the $SU(3)_L$ symmetry is $1.7\,\mathrm{TeV} < w < 2.2\,\mathrm{TeV}$, and in this range, the anomalous muon magnetic moment can be explained

$$(\Delta a_\mu)_{\mathrm{EXP\text{-}SM}} = (26.1 \pm 8) \times 10^{-10}. \qquad (2.9)$$

12

The LHC constraint for mass of Z' in the S331 model reads $w > 2.38$ TeV, and is very close to the parameter space of w that brings appropriate explanation for $(\Delta a_\mu)_{EXP-SM}$. In other words, in the parameter space explaining LHC result, the value of the anomalous muon magnetic moment is predicted, $(\Delta a_\mu)_{331} < 13.8 \times 10^{-10}$. This limit is very close to the constraint given in (2.9).

2.3. QFV interactions of Higgs

2.3.1. Meson mixing systems

FCNC is caused not only by the exchange of the new neutral gauge boson (Z'), but also by the exchange of SM's Higgs boson and the new Higgs boson.

$$\mathcal{L}_Y \supset \bar{u}'_R \mathcal{G}_h^u u'_L h + \bar{d}'_R \mathcal{G}_h^d d'_L h + \bar{u}'_R \mathcal{G}_H^u u'_L H + \bar{d}'_L \mathcal{G}_H^d d'_R H + h.c. \quad (2.10)$$

with $\mathcal{G}_h^u = -\left(V_R^u\right)^\dagger \left\{ c_\xi \frac{1}{u} M^u + s_\xi \frac{h^u}{\Lambda} \frac{u}{2} \right\} V_L^u$, $\mathcal{G}_h^d = -\left(V_R^d\right)^\dagger \left\{ c_\xi \frac{1}{u} M^d - s_\xi \frac{h^d}{\Lambda} \frac{u}{2} \right\} V_L^d$, $\mathcal{G}_H^u = -\left(V_R^u\right)^\dagger \left\{ s_\xi \frac{1}{u} M^u - c_\xi \frac{h^u}{\Lambda} \frac{u}{2} \right\} V_L^u$, and $\mathcal{G}_H^d = -\left(V_R^d\right)^\dagger \left\{ s_\xi \frac{1}{u} M^d + c_\xi \frac{h^d}{\Lambda} \frac{u}{2} \right\} V_L^d$.

The study of FCNC is associated with Z'_μ leading to $m_{Z'} > 4.67$ TeV . This limit is close to the Landau pole, the point at which the theory loses renormalizability. With the choice $(V_{dL})_{3a} = 0$, we have only FCNC associated Higgs,s which will be constrained by measurements of meson mixing systems K^0 and $B_{s,d}^0$,

$$
\begin{aligned}
\mathcal{L}_{FCNC}^{eff} =\ & \left\{ \frac{\left[(\mathcal{G}_h^q)_{ij}\right]^2}{m_h^2} + \frac{\left[(\mathcal{G}_H^q)_{ij}\right]^2}{m_H^2} \right\} (\bar{q}_{iR} q_{jL})^2 \\
& + \left\{ \frac{\left[(\mathcal{G}_h^q)_{ji}^*\right]^2}{m_h^2} + \frac{\left[(\mathcal{G}_H^q)_{ji}^*\right]^2}{m_H^2} \right\} (\bar{q}_{iL} q_{jR})^2 \\
& + 2 \left\{ \frac{\left[(\mathcal{G}_h^q)_{ij}\right]}{m_h} + \frac{\left[(\mathcal{G}_H^q)_{ij}\right]}{m_H} \right\} \left\{ \frac{\left[(\mathcal{G}_h^q)_{ji}^*\right]}{m_h} + \frac{\left[(\mathcal{G}_H^q)_{ji}^*\right]}{m_H} \right\} \\
& \times (\bar{q}_{iR} q_{jL})(\bar{q}_{iL} q_{jR}) .
\end{aligned}
\quad (2.11)
$$

We consider the ratio $\kappa \equiv \frac{\left[(\mathcal{G}_h^q)_{ij}\right]^2 m_H^2}{\left[(\mathcal{G}_H^q)_{ij}\right]^2 m_h^2} \simeq \frac{m_H^2}{m_h^2} \tan^2 \xi < 1$ for $w >> u$. This suggests that the new scalar Higgs H gives more contributions FCNC than

SMLHB h. The strongest constraint for New Physics coming from the system B_s–$\bar{B}_s$, it leads the limit of $(\mathcal{G}_h^q)_{32}$ as :

$$2\left(1+\frac{1}{\kappa}\right)|(\mathcal{G}_h^q)_{32}|^2 = 2\left(1+\frac{1}{\kappa}\right)\frac{\lambda_3^2 u^4}{\lambda_2^2 w^4}|\left[(V_R^d)^\dagger h^d V_L^d\right]_{23}|^2 < 1.8 \times 10^{-6} \quad (2.12)$$

When $\lambda_3/\lambda_2 > 1$ and V_R^d, h^d are matched, the new physical scale can be chosen to be positioned away from the Landau pole.

2.3.2. $h \to q_i q_j$

The S331 model predicts the branching ratio $\mathrm{Br}(h \to q_i q_j)$ as shown in the Table 2.1. The weakest constraint comes from b–s, $\mathrm{Br}(h - b\bar{s}) < 3.5 \times 10^{-3}$, which is too small to search at LHC because of the large QCD background, but these signals are expected to be observed in the near future at ILC.

Observables	Constraints
Oscillation D^0	$\mathrm{Br}(h \to u\bar{c}) \leq \frac{2\times 10^{-4}}{1+\frac{1}{\kappa}}$
Oscillation B_d^0	$\mathrm{Br}(h \to d\bar{b}) \leq \frac{8\times 10^{-5}}{1+\frac{1}{\kappa}}$
Oscillation K^0	$\mathrm{Br}(h \to d\bar{s}) \leq \frac{2\times 10^{-6}}{1+\frac{1}{\kappa}}$
Oscillation B_s^0	$Br(h \to s\bar{b}) \leq \frac{7\times 10^{-3}}{1+\frac{1}{\kappa}}$

Table 2.1: The upper bound for the flavor violation decays of SMLHB to light quarks with a confidence level of 95% from the measurements of meson mixing systems.

2.3.3. $t \to qh$ $(q = u, c)$

The quark flavor violating interactions of SMLHB in the Eq. (2.10) also lead to the non standard decays of top quark $t \to hu_i$, $u_i = u, c$,

$$\mathrm{Br}(t \to u_i h) \simeq \frac{\Gamma(t \to u_i h)}{\Gamma(t \to bW^+)}, \quad \Gamma(t \to hu_i) = \frac{|\mathcal{G}_{i3}^u|^2 + |\mathcal{G}_{3i}^u|^2}{16\pi}\frac{\left(m_t^2 - h_h^2\right)^2}{m_t^3} \quad (2.13)$$

The LHC searches for $\mathrm{Br}(t \to hc) < 0.16\%$ and $\mathrm{Br}(t \to hu) < 0.19\%$ with a confidence level of 95%. In Fig. 2.5, we draw $\mathrm{Br}(t \to hc)$ when fixing $\left[(V_R^u)^\dagger h^u V_L^u\right]_{32} = \left[(V_R^u)^\dagger h^u V_L^u\right]_{23} = 2\frac{\sqrt{m_c m_t}}{u}$. $\mathrm{Br}(t \to ch)$ can be reached at 10^{-3} if the new physics scale is about a few hundred GeV, and the factor $\frac{\lambda_3}{\lambda_2} > 5$. In this

14

parameter space, the mixing angle ξ is large. $\text{Br}(t \to ch)$ decreases quickly when the factor $\frac{w}{u}$ increases. With small mixing angle ξ, $\text{Br}(t \to ch)$ changes from 10^{-5} to 10^{-8}.
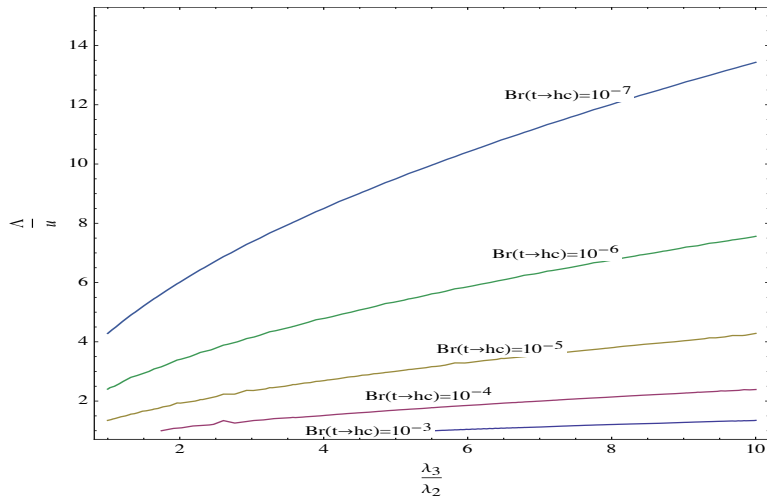

Figure 2.5: The branching ratio of top quark decays to hc.

2.4. Conclusions

We study constraints from the phenomenologies related to the flavor violating Yukawa interactions in the S331 model.

Both Higgs triplets couple with leptons and quarks, causing flavor violating signals in both lepton and quark sectors. We have pointed out that this model provides large enough branching ratio for the lepton flavor violation decay of SMLHB $h \to \mu\tau$, and also agrees with other experimental constraints, including $\tau \to \mu\gamma$ and $(g-2)_\mu$.

The FCNC interactions, Higgs–quark–quark interactions, and meson mixing systems are discussed. $\text{Br}(h \to qq')$ can be enhanced via the measurement of the meson mixing systems. The branching ratio of $t \to qh$ can reach 10^{-3}, but also as low as 10^{-8}.

15

CHAPTER 3. PHYSICAL CONSTRAINTS DERIVED FROM FCNC INTERACTIONS IN THE 3-3-1-1 MODEL

3.1. The summary of the 3-3-1-1 model

The gauge symmetry group is $SU(3)_C \times SU(3)_L \times U(1)_X \times U(1)_N$, the electrical and $B - L$ operators are

$$Q = T_3 + \beta T_8 + X, \quad B - L = \beta' T_8 + N, \tag{3.1}$$

Leptons and quarks are arranged as follows:

$$
\begin{aligned}
\psi_{aL} &= (\nu_{aL}, e_{aL}, (N_{aR})^c)^T \sim (1, 3, -1/3, -2/3), \\
\nu_{aR} &\sim (1, 1, 0, -1), \quad e_{aR} \sim (1, 1, -1, -1), \\
Q_{\alpha L} &= (d_{\alpha L}, -u_{\alpha L}, D_{\alpha L})^T \sim (3, 3^*, 0, 0), \\
Q_{3L} &= (u_{3L}, d_{3L}, U_L)^T \sim (3, 3, 1/3, 2/3), \\
u_{aR} &\sim (3, 1, 2/3, 1/3), \quad d_{aR} \sim (3, 1, -1/3, 1/3), \\
U_R &\sim (3, 1, 2/3, 4/3), \quad D_{aR} \sim (3, 1, -1/3, -2/3), \tag{3.2}
\end{aligned}
$$

with $a = 1, 2, 3$, $\alpha = 1, 2$ are the generation indexes. The scalar spectrum is

$$
\begin{aligned}
\eta^T &= (\eta_1^0, \eta_2^-, \eta_3^0)^T \sim (1, 3, -1/3, 1/3), \\
\rho^T &= (\rho_1^+, \rho_2^0, \rho_3^+)^T \sim (1, 3, 2/3, 1/3), \\
\chi^T &= (\chi_1^0, \chi_2^-, \chi_3^0)^T \sim (1, 3, -1/3, -2/3), \quad \phi \sim (1, 1, 0, 2). \tag{3.3}
\end{aligned}
$$

Their corresponding VEVs are

$$< \eta_1^0 >= \frac{u}{\sqrt{2}}, \quad < \rho_2^0 >= \frac{v}{\sqrt{2}}, \quad < \chi_3^0 >= \frac{w}{\sqrt{2}}, \quad < \phi >= \frac{\Lambda}{\sqrt{2}}. \tag{3.4}$$

The VEVs, u, v, break the electroweak symmetry and generate masses for the SM's particles with the following condition: $u^2 + v^2 = 246^2$ GeV^2. The remaining VEVs, w, Λ, break $SU(3)_L, U(1)_N$ and generate the masses for the new particles. To be consistent with SM, we propose $w, \Lambda \gg u, v$.

3.2. Rare processes mediated by new gauge bosons and new scalars at the tree level

3.2.1. The meson mixing systems

Due to the different arrangement between the generations of quarks, SM quarks couple both Higgs triplets, leading to the FCNC associated neutral Higgs at the tree level, along with new gauge bosons $Z_{2,N}$. We are now looking at how the FCNCs caused by new gauge bosons and new scalars affect the meson oscillation systems in the 3-3-1-1 model. The difference masses of mesons can be split as the sum of SM and new physics contributions (see in the thesis for details)

$$\Delta m_{K,B_d,B_s} = (\Delta m_{K,B_d,B_s})_{\text{SM}} + (\Delta m_{K,B_d,B_s})_{\text{NP}}, \qquad (3.5)$$

We have the following constraints between new physics and experiments

$$-0.3 < \frac{(\Delta m_K)_{\text{NP}}}{(\Delta m_K)_{\text{exp}}} < 0.3, -0.4 < \frac{(\Delta m_{B_d})_{\text{NP}}}{(\Delta m_{B_d})_{\text{SM}}} < 0.17, \ -0.29 < \frac{(\Delta m_{B_s})_{\text{NP}}}{(\Delta m_{B_s})_{\text{SM}}} < 0.2. \ (3.6)$$

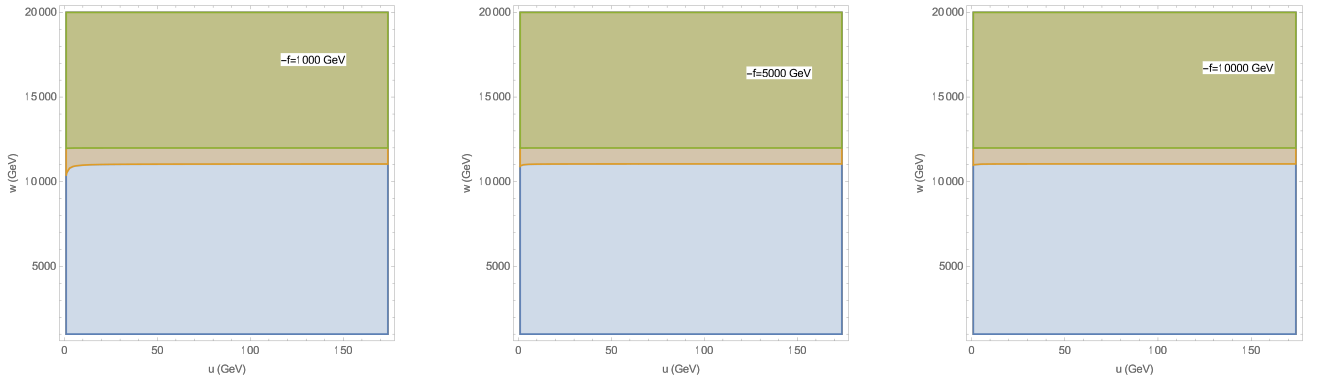Figure 3.1: The constraints for both w and u obtained from the differences of meson masses Δm_K, Δm_{B_s} and Δm_{B_d}. The allowable region for Δm_K is whole panel, whereas the orange and green regimes are for Δm_{B_s} and Δm_{B_d}.

The Fig. 3.1 shows the mixing parameters that are less affected by FCNC induced by new scalars.

Next, we compare the contributions by FCNC associated with new gauge bosons and new scalars to meson mixing parameters, shown in Fig. 3.2. As a result, the primary contribution comes from FCNC associated with new gauge bosons.

In Fig. 3.1, we obtain the lower bound for the new physics scale satisfying constraints (3.6), $w > 12$ TeV. This limit is much tighter and remarkably larger

than the previously obtained limit, since in the previous studies, the authors ignored the SM contributions and just compared the New Physics prediction with measurements.
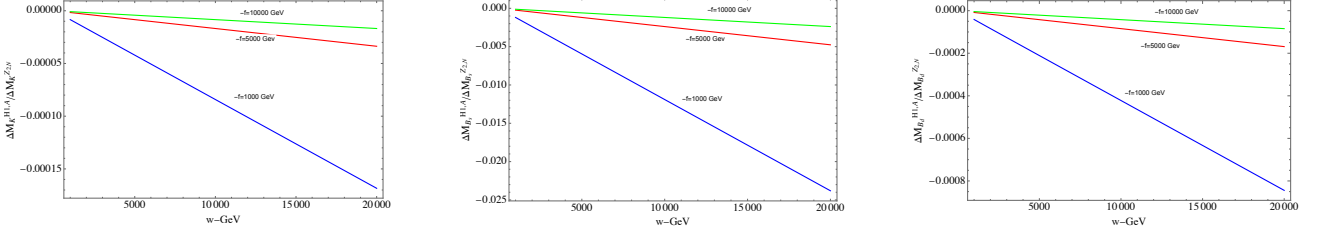

Figure 3.2: The figure illustrates the dependence of the ratio $\Delta m_{K,B_s,B_d}^{H_1,A}/\Delta m_{K,B_s,B_d}^{Z_2,Z_N}$ on the new physics scale w.

3.2.2. $B_s \to \mu^+\mu^-$, $B \to K^*\mu^+\mu^-$ and $B^+ \to K^+\mu^+\mu^-$

The effective Hamiltonian for the processed $B_s \to \mu^+\mu^-$, $B \to K^*\mu^+\mu^-$ and $B^+ \to K^+\mu^+\mu^-$ are

$$\mathcal{H}_{\text{eff}} = -\frac{4G_F}{\sqrt{2}}V_{tb}V_{ts}^* \sum_{i=9,10,S,P} \left(C_i(\mu)\mathcal{O}_i(\mu) + C_i'(\mu)\mathcal{O}_i'(\mu)\right), \quad (3.7)$$

Their corresponding Wilson coefficients contain both SM and new physics contributions at the tree level

$$C_9^{\text{NP}} = -\Theta_{23}\frac{m_W^2}{c_W V_{tb}V_{ts}^*}\frac{(4\pi)^2}{e^2}\left(\frac{g_2}{g}\frac{g_V^{Z_2}(f)}{m_{Z_2}^2} + \frac{g_N}{g}\frac{g_V^{Z_N}(f)}{m_{Z_N}^2}\right),$$

$$C_{10}^{\text{NP}} = \Theta_{23}\frac{m_W^2}{c_W V_{tb}V_{ts}^*}\frac{(4\pi)^2}{e^2}\left(\frac{g_2}{g}\frac{g_A^{Z_2}(f)}{m_{Z_2}^2} + \frac{g_N}{g}\frac{g_A^{Z_N}(f)}{m_{Z_N}^2}\right). \quad (3.8)$$

It is worth noting that $C_{\text{S,P}}^{\text{SM}} = C_{\text{S,P}}'^{\text{SM}} = 0$. Hence, $C_{\text{S,P}}, C_{\text{S,P}}'$ obtained by the New Physics contributions as follows:

$$C_S^{\text{NP}} = \frac{8\pi^2}{e^2}\frac{1}{V_{tb}V_{ts}^*}\frac{\Gamma_{23}^d\Gamma_{\alpha\alpha}^l}{m_{H_1}^2}, \qquad C_S'^{\text{NP}} = \frac{8\pi^2}{e^2}\frac{1}{V_{tb}V_{ts}^*}\frac{\left(\Gamma_{32}^d\right)^*\Gamma_{\alpha\alpha}^l}{m_{H_1}^2},$$

$$C_P^{\text{NP}} = -\frac{8\pi^2}{e^2}\frac{1}{V_{tb}V_{ts}^*}\frac{\Gamma_{23}^d\Delta_{\alpha\alpha}^l}{m_A^2}, \qquad C_P'^{\text{NP}} = \frac{8\pi^2}{e^2}\frac{1}{V_{tb}V_{ts}^*}\frac{\left(\Gamma_{32}^d\right)^*\Delta_{\alpha\alpha}^l}{m_A^2}, \quad (3.9)$$

where $\Gamma_{\alpha\alpha}^l = \Delta_{\alpha a}^l = \frac{u}{v}m_{l_\alpha}$. The branching ratio for the decay $B_s \to l_\alpha^+ l_\alpha^-$ reads

$$\text{Br}(B_s \to l_\alpha^+ l_\alpha^-)_{\text{theory}} = \frac{\tau_{B_s}}{64\pi^3}\alpha^2 G_F^2 f_{B_s}^2 |V_{tb}V_{ts}^*|^2 m_{B_s}\sqrt{1 - \frac{4m_{l_\alpha}^2}{m_{B_s}^2}}$$

18

$$\times \left\{ \left(1 - \frac{4m_{l_\alpha}^2}{m_{B_s}^2}\right) \left| \frac{m_{B_s}^2}{m_b + m_s}(C_S - C_S') \right|^2 \right. \tag{3.10}$$

$$\left. + \left| 2m_{l_\alpha}(C_{10} - C_{10}') + \frac{m_{B_s}^2}{m_b + m_s}(C_P - C_P') \right|^2 \right\},$$

If the oscillation effect of the system $B_s - \bar{B}_s$ is considered, the predicted value of theory and experiment will be related by

$$\mathrm{Br}(B_s \to l_\alpha^+ l_\alpha^-)_{\mathrm{exp}} \simeq \frac{1}{1 - y_s} \mathrm{Br}(B_s \to l_\alpha^+ l_\alpha^-)_{\mathrm{theory}}, \tag{3.11}$$

For $B_s \to e^+ e^-$, SM prediction and current experimental limit are

$$\mathrm{Br}(B_s \to e^+ e^-)_{\mathrm{SM}} = (8.54 \pm 0.55) \times 10^{-14}, \quad \mathrm{Br}(B_s \to e^+ e^-)_{\mathrm{exp}} < 2.8 \times 10^{-7} \tag{3.12}$$

The SM prediction for the branching ratio of $B_s \to e^+ e^-$ is very suppressed by the upper experimental constraint. This is a potentially useful channel for searching for new physics signals. In contrast with $B_s \to e^+ e^-$, the very recent measurement result for the branching ratio of $B_s \to \mu^+ \mu^-$ is

$$\mathrm{Br}(B_s \to \mu^+ \mu^-)_{\mathrm{exp}} = (3.09^{+0.46\;+0.15}_{-0.43\;-0.11}) \times 10^{-9}. \tag{3.13}$$

Whereas, the SM predicts

$$\mathrm{Br}\left(B_s \to \mu^+ \mu^-\right)_{\mathrm{SM}} = (3.66 \pm 0.14) \times 10^{-9}. \tag{3.14}$$
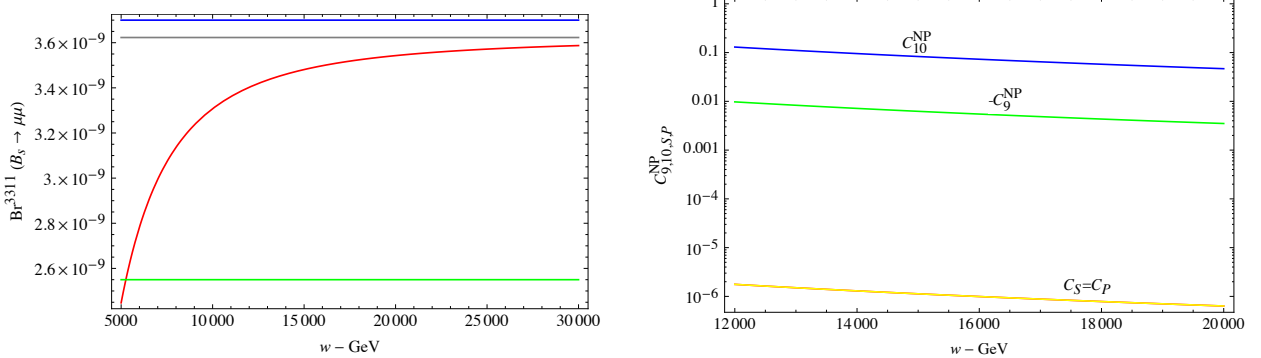

Figure 3.3: The left panel plots $\mathrm{Br}(B_s \to \mu^+ \mu^-)$: the red curve line shows the prediction value of the 3-3-1-1 model, and the gray line shows the central value of the SM prediction. The blue and green lines represent, respectively, the upper and lower bounds of measurement. The right panel predicts the new physics contributions to the Wilson coefficients. Both panels are plotted by fixing $\Lambda = 1000w, f = -w, u = 200$ GeV. Other input parameters are chosen for the section 3.2

From Fig. 3.3, we have $w > 5$ TeV, lower than the obtained limit. Hence, the limit satisfying both the meson mixing system $(\bar{B}_s - B_s)$ and $\text{Br}(B_s \to \mu^+\mu^-)$ is $w > 12$ TeV. In the right panel of Fig. 3.3, $C_{9,10}^{\text{NP}} >> C_{\text{S,P}}$. For $w > 12$ TeV, $C_{10}^{\text{NP}} > 0$, $\text{Br}(B_s \to \mu^+\mu^-)$ reduces about 5%, bringing the prediction value and experimental value close to each other.

The anomalies in $B \to K^*\mu^+\mu^-$ can be explained if $C_9^{\text{NP}} \simeq -1.1$. With the following constraint $w > 12$ TeV, $C_9^{\text{NP}} \simeq -0.01$. Hence, the model 3-3-1-1 cannot deal with the anomalies in decay of $B \to K^*\mu^+\mu^-$.

Both two Wilson coefficients C_9, C_{10} account for $\text{Br}\,(B^+ \to K^+\mu^+\mu^-)$. As predicted by the 3-3-1-1 model, $w > 12$ TeV, C_9^{NP} and C_{10}^{NP} are too tiny, hence the anomalies in the decay $B^+ \to K^+\mu^+\mu^-$ also cannot be interpreted in the 3-3-1-1 model.

3.3. The radiative decays

3.3.1. $b \to s\gamma$

Apart from the charged currents induced by the SM gauge bosons, $W_\mu^\pm$, the 3-3-1-1 model also provides new charged currents, which couple with the new gauge boson $Y_\mu^\pm$, two new charged Higgs $H_4^\pm, H_5^\pm$, và and FCNC associated by $Z_{2,N}$. All of these currents contribute to the decay $b \to s\gamma$.

The effective Hamiltonian for the decay $b \to s\gamma$ reads

$$\mathcal{H}_{\text{eff}}^{b \to s\gamma} = -\frac{4G_F}{\sqrt{2}} V_{tb}V_{ts}^*[C_7(\mu_b)\mathcal{O}_7 + C_8(\mu_b)\mathcal{O}_8 + C_7'(\mu_b)\mathcal{O}_7' + C_8'(\mu_b)\mathcal{O}_8'], \quad (3.15)$$

The Wilson coefficients $C_{7,8}(\mu_b)$ can be split as : $C_{7,8}(\mu_b) = C_{7,8}^{\text{SM}}(\mu_b) + C_{7,8}^{\text{NP}}(\mu_b)$. The New Physics contributes to $C_{7,8}^{\text{NP}}$ via one-loop diagrams (see in the thesis for details)

The index 0 indicates that these Wilson coefficients have not considered QCD corrections. It is important to stress that QCD corrections for $b \to s\gamma$ are essential and have to be included. At the scale $\mu \sim m_b$, $w = 10$ TeV, we have $C_7^{Z_{2,N}}(\mu_b) \simeq \mathcal{O}(10^{-5})$, much smaller compared with SM one, $C_7^{\text{SM}}(\mu_b) = -0.3523$. Consequently, in our calculation, $C_7^{Z_{2,N}}$ can be ignored. The QCD corrections for C_7^Y and $C_7^{H_5}$ at the leading order (LO) are

$$C_7^Y(\mu_b) = \kappa_7 C_7^Y(m_Y) + \kappa_8 C_8^Y(m_Y), \quad C_7^{H_5}(\mu_b) = \kappa_7 C_7^{H_5}(m_Y) + \kappa_8 C_8^{H_5}(m_Y) \quad (3.16)$$

The branching ratio $\text{Br}(b \to s\gamma)$ is given by

$$\text{Br}(b \to s\gamma) = \frac{6\alpha}{\pi C} \frac{|V_{ts}^* V_{tb}|^2}{|V_{cb}|^2}(|C_7(\mu_b)|^2 + N(E_\gamma))\text{Br}(b \to ce\bar{\nu}_e), \quad (3.17)$$
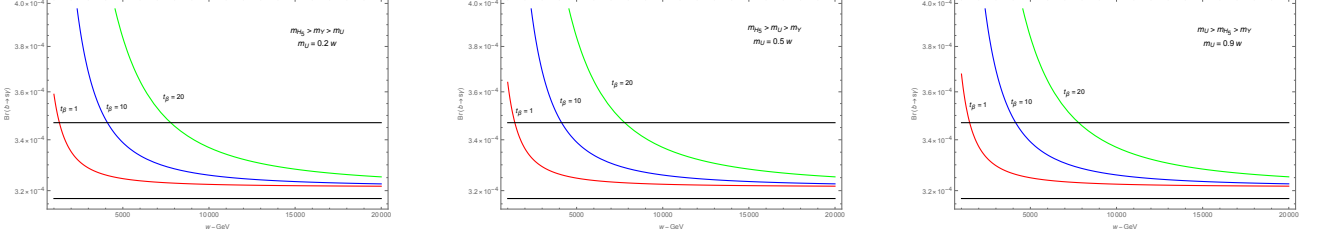
20

Figure 3.4: The dependence of $\mathrm{Br}(b \to s\gamma)$ on the new physics scale w, in the limit $u, v \ll -f\frac{u^2+v^2}{uv} \sim w \sim \Lambda$. The dashed black line shows the current experimental constraints $\mathrm{Br}(b \to s\gamma) = (3.32 \pm 0.15) \times 10^{-4}$

.

In Fig. 3.4, we realize that the branching ratio is strongly affected by the value of t_β, whereas the term containing t_β comes from the $C_7^{H_5}$. The lower bound of the new physics scale depends on t_β, namely, $w \geq 1$ TeV for $t_\beta = 1$; $w \geq 4.1$ TeV for $t_\beta = 10$; $w \geq 7.7$ TeV for $t_\beta = 20$. These bounds are lower than the bounds obtained in the previous sections.

Similarly, we plot $\mathrm{Br}(b \to s\gamma)$ in the scenario $u, v \ll -f \sim w \sim \Lambda$ in Fig. 3.5. We see that the dependence of the branching ratio on t_β is not as strong as in Fig. 3.4. In the condition $w > 12$ TeV, the influence of t_β to $\mathrm{Br}(b \to s\gamma)$ becomes insignificant, and the predicted value of the model is close to the central value of measurement.
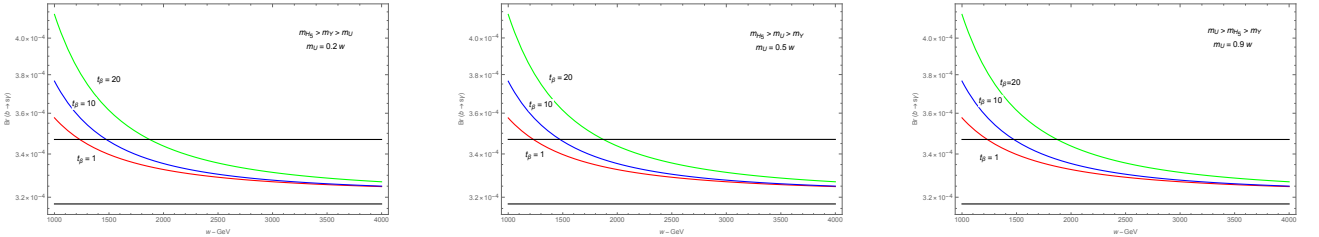

Figure 3.5: The dependence of $\mathrm{Br}(b \to s\gamma)$ on the new physics scale w in the case $u, v \ll -f \sim w \sim \Lambda$.

cLFV decay

The 3-3-1-1 model contains some new charged currents coupled with new charged particles $Y^\pm, H_{4,5}^\pm$, which give contributions to cLFV. The branching ratio $\mathrm{Br}(\mu \to e\gamma)$ is

$$\mathrm{Br}(\mu \to e\gamma) = \frac{12\pi^2}{G_F^2}(|A_L|^2 + |A_R|^2)\mathrm{Br}(\mu \to e\tilde{\nu}_e\nu_\mu), \qquad (3.18)$$

21

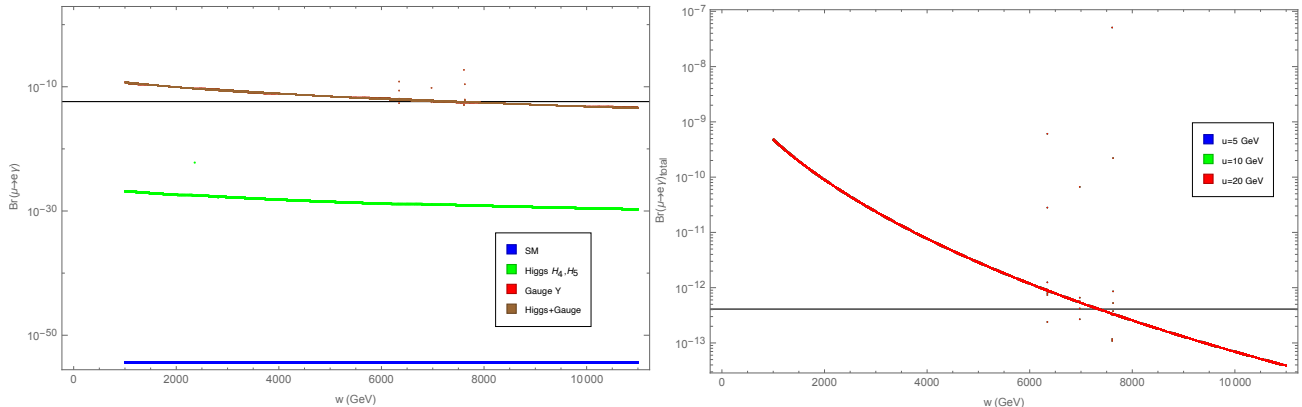where the factors A_L, A_R are expressed detail in the thesis.

Figure 3.6: The numerical result for the branching ratio $\text{Br}(\mu \to e\gamma)$ as the function of the new physics scale w. The black line indicated the experimental upper bound.

The left panel of Fig. 3.6 estimates the magnitude of each contributions to $\text{Br}(\mu \to e\gamma)$. The primary contribution comes from newly charged gauge boson $Y^{\pm}$. In order to satisfy the experimental constraint, the new physic scale needs $w > 7.3$ TeV, and this bound is quite similar to the one obtained when studying the decay $b \to s\gamma$. The right panel of Fig. 3.6 shows $\text{Br}(\mu \to e\gamma)_{\text{total}}$ depends very slightly on u. It is worth noting that the factors $A_{L,R}^{H_4, H_5}$ are affected by the electroweak scales u and v. Therefore, this result suggests that the charged current and associated new charged Higgs have insignificant impacts on the decay $\mu \to e\gamma$ and can be ignored.

3.4. Conclusions

In the 3-3-1-1 model, we study some phenomenologies related to FCNC. The sources of the tree level FCNC come from both gauge bosons and Higgs, as clarified. The experiments for meson oscillations will constrain the tree level FCNC tightly. The obtained lower bound of the new physics scale is stronger than before, $M_{\text{new}} > 12$ TeV.

In this limit, the tree level FCNC gives negligible contributions to $\text{Br}(B_s \to \mu^+\mu^-)$, $\text{Br}(B \to K^*\mu^+\mu^-)$ and $\text{Br}(B^+ \to K^+\mu^+\mu^-)$. The branching ratio of the radiative decay $b \to s\gamma$ is affected by the factor $\frac{v}{u}$ via the diagrams mediated by the newly charged Higgs. In contrast, the new charged current induced by the new gauge boson $Y_\mu^{\pm}$ gives the main contribution to the process $s\mu \to e\gamma$.

GENERAL CONCLUSION

THE EFFECT OF SCALAR FIELDS ON THE FLAVOR-CHANGING NEUTRAL CURRENTS IN THE S331 MODEL AND 3-3-1-1 MODEL

A. The S331 model: We study the constraints from some phenomenology associated with Yukawa interactions flavor-violating in the S331 model.

- Both Higgs triplets interact with leptons and quarks, causing flavor-violating signals in the leptons and quarks sector. We have shown that this model can give large contribution to LFVHD $h \to \mu\tau$ and can reach agreement with other experimental constraints, such as cLFV decay $\tau \to \mu\gamma$ and anomalous muon magnetic moment $(g-2)_\mu$.

- Contributions of flavor-changing neutral currents, Higgs–quark–quark interactions, meson mixing systems are studied. $\text{Br}(h \to qq')$ can be increased according to the measurement of the meson mixing system, the branching ratio of $t \to qh$ can reach 10^{-3}, but can also be as small as 10^{-8}.

B. The 3-3-1-1 model: In the 3-3-1-1 model, we discuss some of the phenomenology associated with FCNC .

- The source of FCNC at the tree level coming from both the gauge and Higgs bosons is clarified. Experiments for meson oscillations will constrain the tree level FCNC. The lower limit of the newly obtained physic scale is tighter than before, $\text{M}_{\text{new}} > 12$ TeV.

- In this limit, the tree level FCNC gives a negligible contribution to $\text{Br}(B_s \to \mu^+\mu^-)$, $\text{Br}(B \to K^)*\mu^+\mu^-)$ and $\text{Br}(B^+ \to K^+\mu^+\mu^-)$.

- The branching ratio of the radiative decay $b \to s\gamma$ is influenced by the coefficient factor $\frac{v}{u}$ via the diagrams mediated by the newly charged Higgs boson. In contrast, the charged current of the new gauge boson $Y_\mu^\pm$ is the major contributor to the decay process $\mu \to e\gamma$.

NEW FINDINGS OF THE THESIS

1. We study the constraints from some phenomenology associated with Yukawa interactions violating flavor in the S331 model. We have shown that this model can give large contribution to LFVHD $h \to \mu\tau$ and can reach agreement with other experimental constraints, such as $\tau \to \mu\gamma$ and $(g-2)_\mu$. The contributions of the flavor-changing neutral currents interaction, the Higgs–quark–quark interaction, and the meson mixing system are studied. $\mathrm{Br}(h \to qq')$ can be increased according to the measurement of the meson mixing system. The branching ratio of $t \to qh$ can reach 10^{-3}, but can also be as small as 10^{-8}.

2. In the 3-3-1-1 model, we discuss some of the phenomenology associated with FCNC. The source of FCNC at the tree level coming from both the gauge and Higgs bosons is clarified. Experiments for meson oscillations will constrain the tree level FCNC. The lower limit of the newly obtained physic scale is tighter than before, $\mathrm{M_{new}} > 12$ TeV. In this limit, the tree level FCNC gives a negligible contribution to $\mathrm{Br}(B_s \to \mu^+\mu^-)$, $\mathrm{Br}(B \to K^)*\mu^+\mu^-)$ and $\mathrm{Br}(B^+ \to K^+\mu^+\mu^-)$. The branching ratio of the radiative decay $b \to s\gamma$ is influenced by the coefficient factor $\frac{v}{u}$ via the diagrams mediated by the newly charged Higgs boson. In contrast, the charged current of the new gauge boson $Y_\mu^\pm$ is the major contributor to the decay process $\mu \to e\gamma$.

3. It has been shown that the number of flavor-violating proceesed caused by the scalar fields in the two models S331 and 3-3-1-1 are independent of each other. This is explained by the fact that the fermions in these two models receive mass in two different ways: both Higgs triplets generate mass for the fermions in the S331 model, whereas in the 3-3-1-1 model, the fermions have the mass by individual Higgs triplets.

LIST OF PUBLICATIONS

1. D. T. Huong, P. V. Dong, N. T. Duy, N. T. Nhuan and L. D. Thien, *Investigation of dark matter in the 3-2-3-1 model*, Physical Review D **98**, 055033, 2018.

2. D. N. Dinh, D. T. Huong, N. T. Duy, N. T. Nhuan, L. D. Thien, and Phung Van Dong, *Flavor changing in the flipped trinification*, Physical Review D **99**, 055005, 2019.

3. D. T. Huong, N. T. Duy, *Investigation of the Higgs boson anomalous FCNC interactions in the simple 3-3-1 model*, European Physical Journal C **80**, 439, 2020.

4. Duy Nguyen Tuan, Takeo Inami, Huong Do Thi, *Physical constraints derived from FCNC in the 3-3-1-1 model*, European Physical Journal C **81**, 813, 2021.

The thesis only uses the last two publications.